Preparation of ZnO/Brucite Functional Composite Powder by the Mechanochemical Method

Huan Shuai[1,2], Jiao Wang[2]*, Fengguo Ren[2]* and Gaoxiang Du[1]*

[1]School of Materials Science and Technology, China University of Geosciences, Beijing, China, [2]School of Basic Education Department or Faculty, Beijing Polytechnic College, Beijing, China

In this experiment, ZnO/brucite composite powder was prepared through the mechanochemical method; further, the properties, particle morphology, and structure of the composite powder were characterized. The results show that mechanical grinding action can promote the production of a large number of surface ions with unsaturated coordination number on the surface of brucite and ZnO particles, thereby promoting hydroxylation of the particle surfaces. The addition of NaOH to the composite system can also aid the further activation of the surface of the brucite and ZnO particles and the formation of more associated hydroxyl groups. Finally, a core–shell composite powder is formed with weak forces such as hydrogen bonds and van der Waals forces as the connecting bonds.
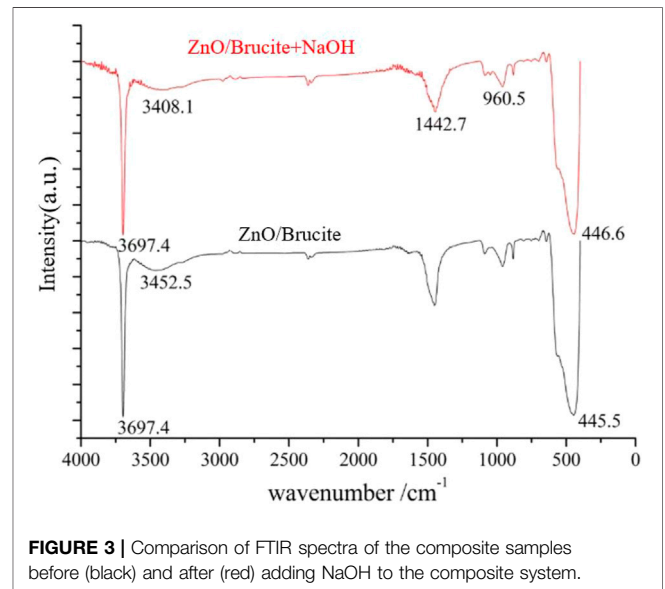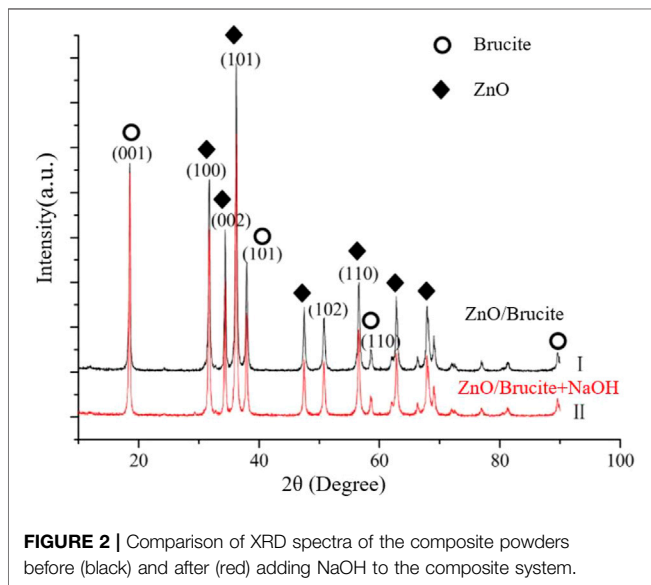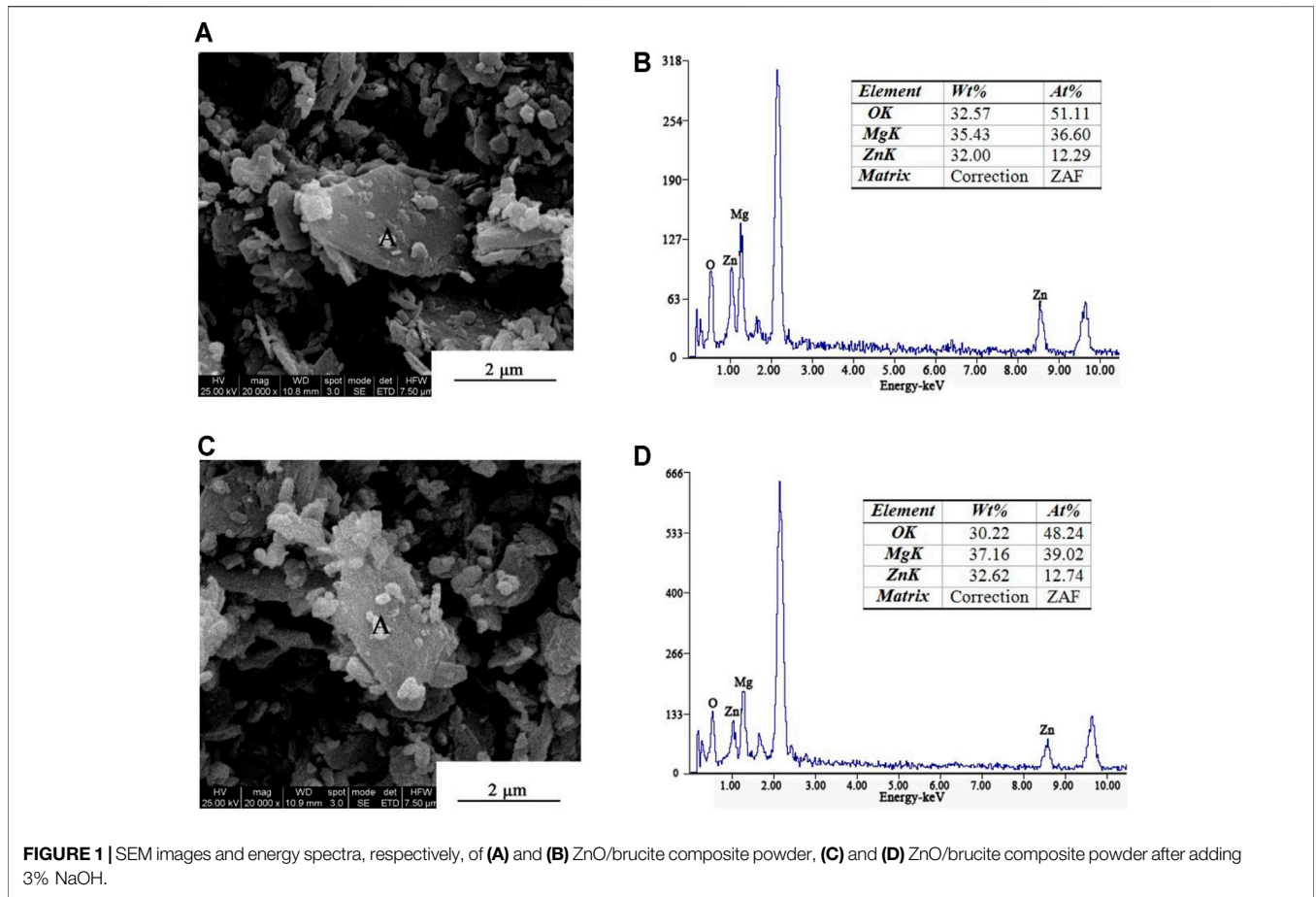
Keywords: brucite, zinc oxide, mechanochemistry, activation, compound

INTRODUCTION

Zinc oxide is an important functional inorganic material in the rubber, ceramics, and coatings industries (Mahla et al., 2021; Kayış et al., 2021). It is especially important in the rubber industry (including rubber tires) because it shortens rubber vulcanization time and significantly improves wear resistance (Suthar et al., 2020; Sreethu and Kinsuk, 2021; Jose and Athikalam Paulose, 2020). However, the application and production process of zinc oxide faces the following problems: 1) The production process has a heavy load, generates serious pollution, and requires a difficult treatment process; 2) insufficient market supply raises the market price of zinc oxide; 3) as the density of zinc oxide is relatively high, the resulting products are also of high density and cannot easily meet the requirements of lightweight materials (Sugavaneshwar and Nanda, 2013). These problems have severely restricted the development of the zinc oxide industry. To reduce the use of zinc oxide, we can coat a zinc-oxide layer on brucite by mechanical grinding (Averin et al., 2019; Pronin et al., 2018; Scepanovic et al., 2006; Wang et al., 2020). As the relative density of brucite (2.3–2.6) is only 40% that of zinc oxide, this method also reduces the density of the composite powder.

The main chemical component of brucite is magnesium hydroxide, a non-metallic mineral with a layered structure (Xu and Wei, 2018; Rui et al., 2014). At high temperatures, brucite decomposes into magnesium oxide and water vapor and exhibits a flame-retardant effect (Wang et al., 2019). Therefore, brucite is a suitable core material with a good coating structure.

The solubilities of brucite and zinc oxide increase under the action of a mechanical force. When the ion concentration of the product adsorbed on the particle surface exceeds the corresponding solubility product constant, the product will recrystallize along the particle surface (Kunio and Meguro, 1975; Lu et al., 2005; Moballegh et al., 2006; Du et al., 2015). If the alkalinity of the composite system is increased during the preparation of the composite powder, the time before brucite

FIGURE 1 | SEM images and energy spectra, respectively, of **(A)** and **(B)** ZnO/brucite composite powder, **(C)** and **(D)** ZnO/brucite composite powder after adding 3% NaOH.

FIGURE 2 | Comparison of XRD spectra of the composite powders before (black) and after (red) adding NaOH to the composite system.

FIGURE 3 | Comparison of FTIR spectra of the composite samples before (black) and after (red) adding NaOH to the composite system.

recrystallization is shortened. Consequently, when brucite particles are subjected to both recrystallization and mechanical grinding, they can undergo dramatic changes in free energy,

which makes the surface of the brucite particles easier to compound with other particles (Tuan et al., 2020). As ZnO is an amphoteric oxide, it will react with NaOH, $ZnO + 2NaOH +$
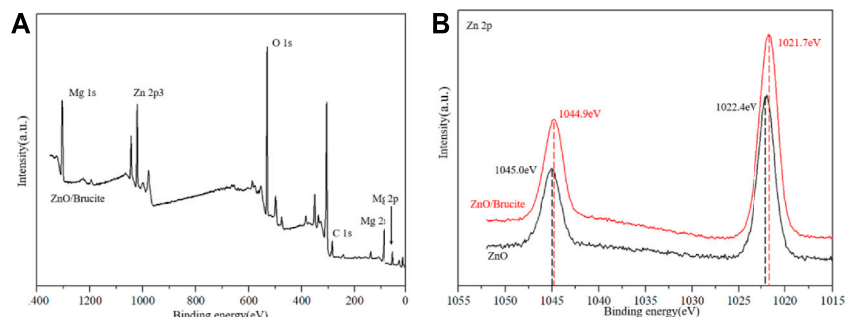
FIGURE 4 | (A) XPS survey spectra of ZnO/Brucite, **(B)** Zn 2p, high-resolution energy spectrum.

$H_2O \rightarrow Na_2[Zn(OH)_4]$, causing further changes in free energy on the ZnO particle surface. Introducing NaOH into the composite system is thus expected to accelerate the composite effect.

In this experiment, ZnO/brucite composite powder was prepared by the mechanochemical method, and the properties, particle morphology, and structure of the composite powder were characterized. Next, the effect of system alkalinity on ZnO/brucite composite powder was studied, and the composite mechanism was analyzed. This study provides theoretical support for the preparation of core–shell composite powders.

RAW MATERIALS AND REAGENTS

Ultra-fine brucite was purchased from Shouchuang Powder Technology Co., Ltd.,Beijing, China. Fifty and ninety percent of the brucite particles are below 4.54 and 9.52 μm in diameter, respectively, and the $Mg(OH)_2$ content is 96.5%. Zinc oxide powder with a ZnO content of 99.6% was purchased from Dalian Zinc Oxide Factory, Shandong, China.

Triethanolamine (TEA) sodium hydroxide was purchased from Beijing Chemical Plant,Beijing, China.

MATERIAL PREPARATION

The functional composite powder of zinc oxide/magnesium hydroxide was prepared by the mechanochemical method as follows:

1) Pretreatment of brucite: The brucite and grinding medium were weighed at a 5:1 ratio of grinding medium to material and distilled water was added to give a slurry concentration of 50%. The materials were combined in a mixing tank. TEA was weighed out and added to brucite raw material (mass ratio = 1%) in the grinding system, and then ground for 3 h at 1,350 rpm.
2) For mechanical activation, zinc oxide was pretreated as described for brucite.
3) Compounding process: The pretreated brucite and mechanically activated zinc oxide were compounded for

3 h at a composite material ratio of 1:1 and a grinding speed of 1,350 rpm. To evaluate the influence of the alkalinity of the system on the composite effect, NaOH was weighed at different set ratios and dissolved in distilled water. The dissolved NaOH was added to the composite system.
4) Filtration and drying: The composite sample was sieved and dried at 110°C. The dried sample was collected for testing.

CHARACTERIZATION

The morphologies and element mass ratios of the composite particles were observed by scanning electron microscopy (SEM) (Quanta 600 FEI, America) and energy spectrum analysis, respectively. The changes in the surface groups of the particles were characterized by Fourier transform infrared spectroscopy (FTIR) (NICOLET 750, America). The changes in crystal structures of the particles were characterized by a P-general XD-3 X-ray diffractometer (XRD) (Beijing, China.) with the following test parameters: Cu–Kα, scanning speed 4°/min, scanning range 15°–90°.

RESULTS AND DISCUSSION

Effect of System Alkalinity on ZnO/Brucite Composite Powder

Panels (a) and (b) of **Figure 1** present the SEM image and energy spectrum of ZnO/brucite composite powder, respectively, while panels (c) and (d) are the SEM image and energy spectrum of ZnO/brucite composite powder prepared with 3% NaOH, respectively. As seen in the SEM images, the brucite particles in both samples are coated with many small particles. The energy spectrum analysis of composite powder A confirms that the coated particles are all ZnO. The weight ratios of Zn and Mg in the ZnO/brucite composite powder are 32.00 and 35.43%, respectively. After adding 3% NaOH, the weight ratios of Zn and Mg in the ZnO/brucite composite powder are 32.62 and 37.16%, respectively. The results show that the amount of ZnO on the brucite particles increases after adding NaOH, and the composite effect is enhanced, indicating that NaOH can promote the preparation of the ZnO/brucite core–shell composite powder to a certain extent.
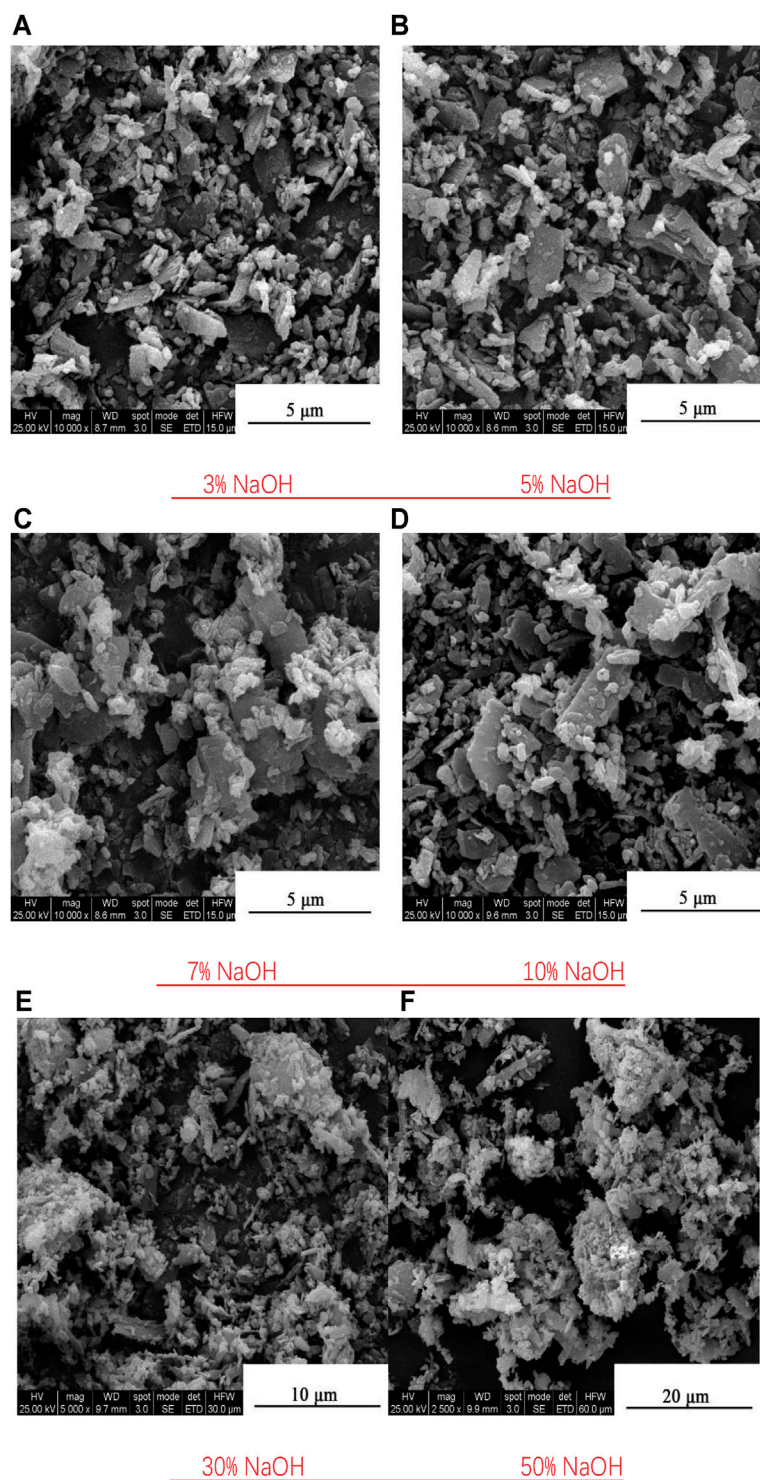
FIGURE 5 | SEM images of composite powders prepared with different amounts of NaOH. **(A)** 3% NaOH **(B)** 5% NaOH **(C)** 7% NaOH **(D)** 10% NaOH **(E)** 30% NaOH **(F)** 50% NaOH.

Figure 2 shows the XRD patterns of the composite powders prepared before and after adding NaOH to the composite system. After the NaOH addition, the intensities of the characteristic peaks of ZnO and brucite decreased and increased, respectively. This result shows that NaOH reacts incompletely with ZnO to generate free $[Zn(OH)_4]^{2-}$ ions. These ions destroy the order of
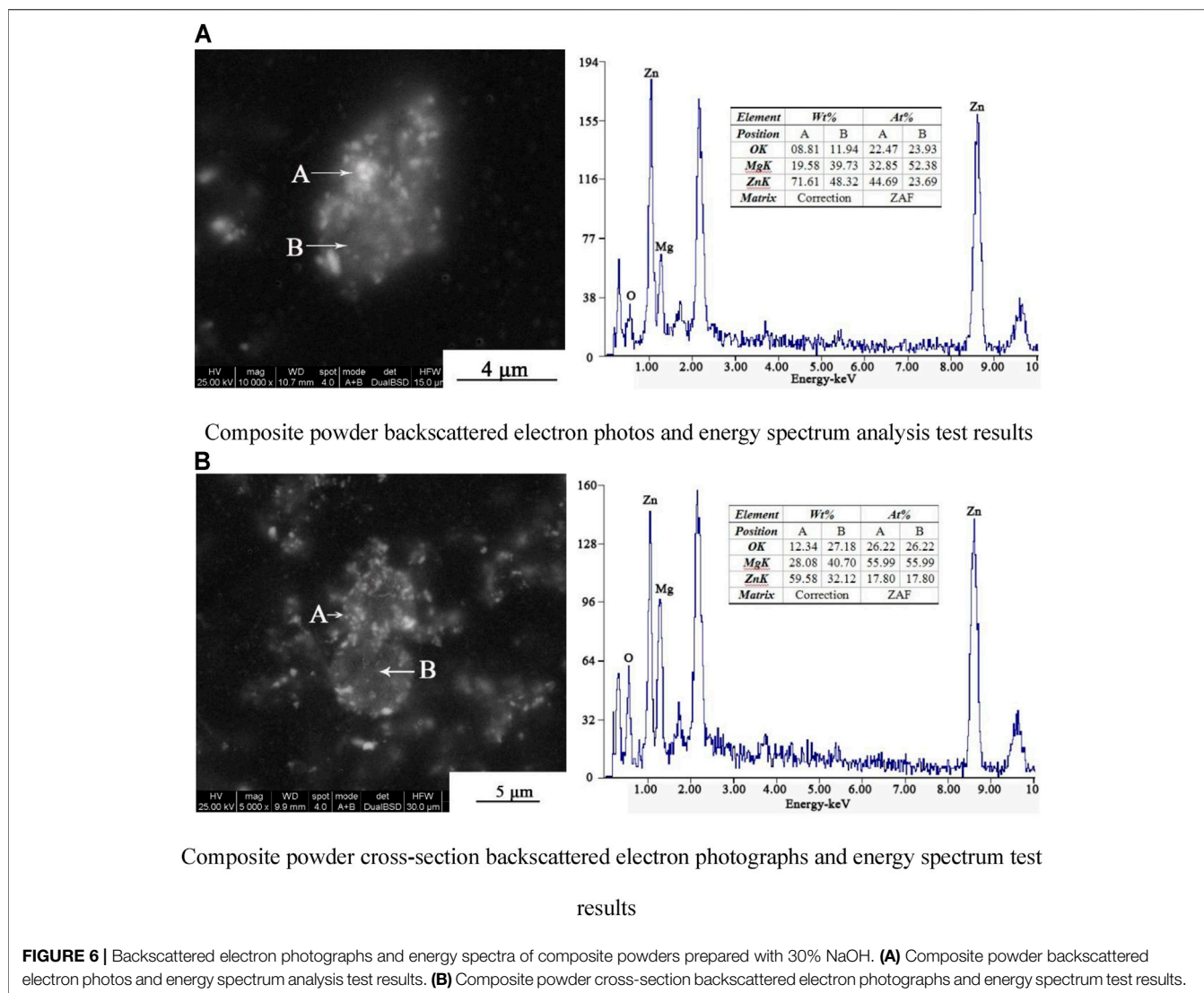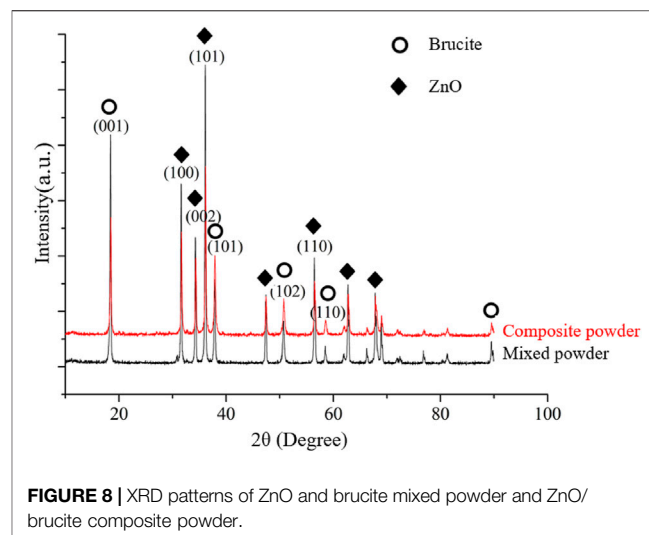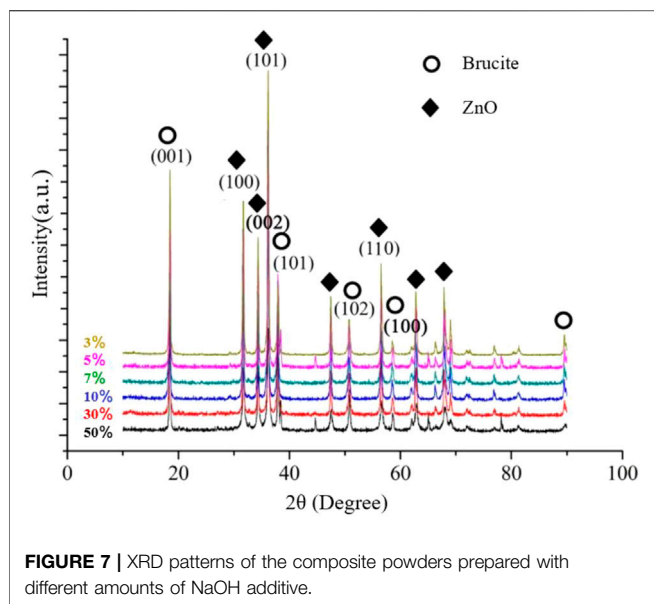
FIGURE 6 | Backscattered electron photographs and energy spectra of composite powders prepared with 30% NaOH. **(A)** Composite powder backscattered electron photos and energy spectrum analysis test results. **(B)** Composite powder cross-section backscattered electron photographs and energy spectrum test results.

the crystal structure of the particles, promoting the formation of associated hydroxyl groups in the ZnO particles. When the OH- concentration in the system increases, the recrystallization phenomenon on the particle surface accelerates and the intensities of the corresponding characteristic peaks increase accordingly.

Figure 3 shows the FTIR spectra of the composite powders. The characteristic peak at 3,697.4 cm^{-1} is attributed to stretching vibrations of the hydroxyl group on the brucite surface. The broad band at 3,452.5 cm^{-1} corresponds to stretching vibrations of the associative hydroxyl groups on the surfaces of the brucite and ZnO particles. The broad absorption peaks at 1,442.7 and 960.5 cm^{-1} are assigned to impurities. The characteristic peaks at 445.5 cm^{-1} are the vibration peaks of the Zn–O and Mg–O bonds, respectively. The wavenumbers of the peaks of brucite and ZnO are relatively similar, so the spectra of both compounds overlap. After adding NaOH to the system, the intensity of the characteristic peak at 3,697.4 cm^{-1} is slightly reduced, probably because NaOH promotes the dehydration and condensation

reactions between hydroxyl groups. Meanwhile, the characteristic peak at 3,452.5 cm^{-1} shifted to 3,408.1 cm^{-1}, indicating that NaOH addition promotes the formation of associated hydroxyl groups on the ZnO and brucite particle surfaces. The hydrogen bonding between the hydroxyl groups is enhanced; this leads to a decrease in the wavenumber of this peak. The characteristic peak at 445.5 cm^{-1} increased to 446.6 cm^{-1}, indicating that NaOH addition slightly increased the energy of the Zn–O and Mg–O bonds. In summary, NaOH can promote the formation of associated hydroxyl groups in the composite system and can increase the energy of the Zn–O and Mg–O bonds to a certain extent, further promoting the composite of the ZnO and brucite.

In order to further analyze the interaction between the ZnO and brucite, XPS is used to test and analyze ZnO/Brucite, and shown in **Figure 4**. **Figure 4B** shows that the Zn 2p at 1,022.4 eV is attributed to the Zn-O bond while the Zn 2p1/2 peak appears at 1,045.0 eV. The distance between the two peaks is 22.6 eV, corresponding to the feature profile of Zn2+ (Jaramillo-Páez

FIGURE 7 | XRD patterns of the composite powders prepared with different amounts of NaOH additive.

FIGURE 8 | XRD patterns of ZnO and brucite mixed powder and ZnO/brucite composite powder.

et al., 2016). The binding energy is reduced, and the Zn and Mg ions have a coordination effect.

To further explore the influence of NaOH on the composite system and determine the optimal amount of NaOH additive, NaOH was added at different proportions (3, 5, 7, 10, 30, and 50%). The SEM images of the resulting composite powders are shown in **Figure 5**.

The composite powders containing 30 and 50% NaOH have stronger composite effects than those with lower NaOH concentration, but increasing the NaOH content aggravates the particle agglomeration. In the compound powder prepared with 50% NaOH, the diameter of the agglomerated particles reaches approximately 20 μm. In the compound powder prepared with 30% NaOH, secondary agglomeration particles are few, and their sizes are less than 10 μm. Most of the composite particles in this sample were dispersed and exhibited a high composite effect. From **Figure 5**, the optimal amount of NaOH additive can be determined as 30%.

Figure 6 shows backscattered electron photographs and energy spectra of the composite powder prepared with 30% NaOH. **Figure 6A** reveals a large number of bright particles outside dark gray particles. The energy spectrum analysis at point A (bright ZnO particles) in **Figure 6A** reveals a Zn weight ratio of 71.61% and an Mg weight ratio of 19.58%. At point B (dark gray brucite particles), the weight ratios of the Zn and Mg elements are 44.69 and 39.73%, respectively. These results can be determined by comparing the contents of Zn and Mg at points A and B. **Figure 6B** reveals a layer of bright particles in the edge area of the dark gray particles, affirming the formation of core–shell coated particles. From the energy spectra, the weight ratios of the Zn and Mg elements are 59.58 and 28.08%, respectively, at point A (bright particles) and 32.12 and 40.70%, respectively, at point B (dark gray particles). Comparing the Zn and Mg contents in the regions of A and B, it can be further determined that the coating material is ZnO and the nucleating material is brucite.

Figure 7 shows the XRD patterns of the composite powders prepared with different NaOH contents. The intensities of the characteristic peaks corresponding to the main crystal planes of ZnO in the composite powder gradually decreases with increasing NaOH amounts, indicating that in the composite system, NaOH gradually reacts with ZnO to generate hydroxylated zinc ions $[Zn(OH)4]^{2-}$ (Uekawa et al., 2004; Lehn et al., 1980). Increasing the amount of added NaOH increases the amount of reactants that damage the ordered structure of the ZnO surface. This damage is reflected in the disordered intensities of the main characteristic peaks of brucite in the composite powder. Increasing the amount of NaOH additive increases the peak intensities of some crystal planes and decreases those of other planes. It was thought that because the crystal faces of brucite have different sizes and densities, they experience different crushing and recrystallization effects. Under the combined action of crushing and recrystallization, The peak intensity changes of the corresponding characteristic peaks of different crystal planes are also different. It can be inferred that the addition of NaOH to the composite system can promote the recrystallization of brucite to a certain extent but also increases the grinding effect on the recrystallized crystal face, further disrupting the crystal structure of the particles. The enhanced activation degree of the particle surfaces further promotes the preparation of the composite powder particles.

To explore the effect of wet mechanical grinding on the preparation of composite powder and the preparation mechanism of composite powder, the composite powder prepared by the mechanochemical method and the powder formed by dispersing and mixing ZnO and brucite under wet conditions were characterized in a comparison study. **Figure 8** compares the XRD patterns of the ZnO/brucite mixed powder and the mechanochemical composite powder. The (100), (002), (101), and (110) planes of ZnO were the main crystal planes after mechanical grinding and incomplete reaction with NaOH. The peak intensities of these peaks after grinding and reaction were reduced by 41.5, 37.2, 42.8, and 46.9%, respectively. During amorphization of the ZnO crystal structure, the mechanical
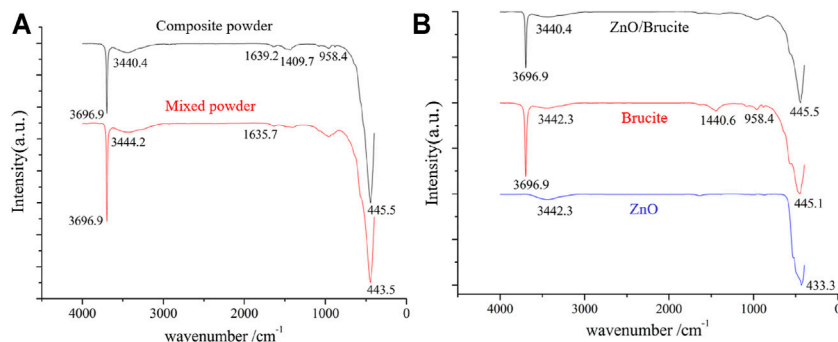
FIGURE 9 | (A), FTIR comparison chart of mixed powder and composite powder; **(B)**, FTIR comparison chart of composite powder and raw materials of brucite and zinc oxide.
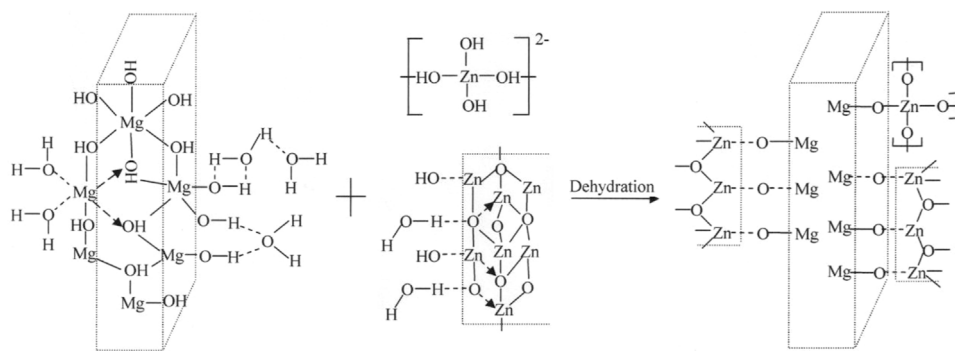

FIGURE 10 | Composite model of brucite, zinc oxide and tetrahydroxy hydrated zinc ion.

energy is converted into surface energy of the particles, which activates the reaction of the ZnO groups on the particle surfaces with NaOH in the aqueous medium. The tetrahydroxy hydrated zinc ions $[Zn(OH)_4]^{2-}$ formed through this reaction reduce the numbers of Zn and O atoms on the ZnO surfaces, further disrupting the ordering of the main crystal faces of ZnO. Consequently, the intensities of the (001), (101), (102), and (110) faces are reduced by 47.7, 4.5, 12.1, and 9.1%, respectively. These results further confirm that mechanical grinding in the composite system can promote the activation of brucite crystal faces.

Figure 9 compares the FTIR spectra of the mixed and composite powders. In **Figure 9A**, the characteristic peak at $3,696.9 \text{ cm}^{-1}$ is attributed to inherent hydroxyl stretching vibrations on the surface of brucite and the broad bands at $3,444.2$ and $1,635.7 \text{ cm}^{-1}$ correspond to stretching and bending vibrations of the associated hydroxyl groups on the surfaces of brucite and zinc oxide, respectively. The broad absorption peaks at $1,409.7$ and 958.4 cm^{-1} are impurity peaks, and the characteristic peaks at 443.5 cm^{-1} belong to vibrations of Zn–O and Mg–O bonds. The wavenumbers of Zn–O and Mg–O were relatively similar, so the spectra overlapped. The characteristic peak at $3,696.9 \text{ cm}^{-1}$ appears in the spectra of both the mixed and composite powders but is more intense in the

latter. The broad bands at $3,444.2$ and $1,635.7 \text{ cm}^{-1}$ in the spectrum of the Mixed powder shifts to $3,440.4$ and $1,639.2 \text{ cm}^{-1}$, respectively, in the spectrum of the Composite powder, affirming that the mechanical forces in the wet grinding system promote the formation of hydroxyl groups on the surfaces of the ZnO and brucite particles. The enhancement of hydrogen bonding results in an increase in the frequency of the stretching vibrations of the associated hydroxyl group and a decrease in the frequency of the bending vibrations. The wavenumbers of the vibration peaks of the Zn–O and Mg–O bonds increased from 443.5 to 445.5 cm^{-1}, indicating that mechanical grinding promotes the crystal-structure changes of brucite and ZnO, hence improving the bond energy of Zn-O bond and Mg-O bond.

After combining ZnO and brucite in the mechanical grinding system (**Figure 9B**), the wavenumber of the characteristic peak remains stable at $3,696.9 \text{ cm}^{-1}$ but its intensity is significantly reduced. The peak of the broad band at $3,444.2 \text{ cm}^{-1}$ reduced to $3,440.4 \text{ cm}^{-1}$. This band was widened and its intensity was reduced, indicating that hydroxyl dehydration condensation occurred between the ZnO and brucite particles in the wet grinding system. Zn---O---Mg bonds were connected *via* hydrogen bonds, van der Waals forces, and other forces that lowered the vibration frequency. The free $[Zn(OH)_4]^{2-}$ ions in the

water medium were affected by the same type of adsorption and were adsorbed on the surfaces of the brucite particles, which consequently became enriched in surface hydroxyl groups. A Zn–O ion membrane then formed through hydroxyl dehydration and condensation between ZnO and brucite in the composite system. This ion membrane may then have formed ZnO. The crystal nucleus gradually grew along the surface of the brucite particles, finally forming a core–shell composite powder. **Figure 10** shows the composite model of brucite, ZnO and $[Zn(OH)4]^{2-}$. The characteristic peaks of ZnO and brucite at 433.3 and 445.1 cm^{-1}, respectively, disappeared in the composite sample, and a new characteristic peak appeared at 445.5 cm^{-1}. The grinding action of the mechanical force likely distorted the crystal lattice of the particles. The electron cloud densities of the Zn–O and Mg–O bonds shifted, leaving the coordination numbers of the Zn, O, and Mg atoms in an unsaturated state. The surface ions with unsaturated coordination numbers interacted with water in the system, further hydroxylating the particle surface and promoting dehydration and condensation between the ZnO and brucite particles.

CONCLUSION

Under mechanical grinding, a large number of ions with unsaturated coordination number were generated on the surfaces of brucite and ZnO particles, which promoted hydroxylation of the particle surfaces. Adding NaOH to the composite system further activated the brucite and ZnO particles and the formation of associated hydroxyl groups. When ZnO/brucite composites were prepared by

mechanochemical methods, dehydration, and condensation of the surface hydroxyl groups between the ZnO and brucite particles occurred, forming Zn---O---Mg bonds connected by weak hydrogen bonds and van der Waals forces. The free tetrahydroxy hydrated zinc ions in the aqueous medium and the surface hydroxyl groups of the brucite particles underwent dehydration and condensation to form a Zn–O ion film. This ionic membrane formed ZnO crystal nuclei, which gradually grew along the surface of the brucite particles and finally formed a core–shell composite powder. The powder prepared by this method has white pigment characteristics, rubber vulcanization accelerator characteristics, antibacterial agent characteristics, flame retardant characteristics and other properties, and can be widely used in rubber and plastic fillers.

DATA AVAILABILITY STATEMENT

The original contributions presented in the study are included in the article/Supplementary Material, further inquiries can be directed to the corresponding authors.

AUTHOR CONTRIBUTIONS

Conceptualization, JW and GD; methodology, HS, JW, and GD; validation, HS, JW, and FR; formal analysis, HS; investigation, HS; data curation, HS; writing—original draft preparation, HS; writing—review and editing, JW, FR, and GD. All authors have read and agreed to the published version of the manuscript.

REFERENCES

Averin, I. A., Pronin, I. A., Yakushova, N. D., Karmanov, A. A., Sychev, M. M., Vikhman, S. V., et al. (2019). Analysis of the Structural Evolution of Zinc Oxide Powders Obtained by Mechanical High-Energy Grinding. *Tech. Phys.* 64 (9), 1330–1335. doi:10.1134/s1063784219090020

Deylam, M., Alizadeh, E., Sarikhani, M., Hejazy, M., and Firouzamandi, M. (2021). Zinc Oxide Nanoparticles Promote the Aging Process in a Size-dependent Manner. *J. Mater. Sci. Mater. Med.* 32 (10), 128. doi:10.1007/s10856-021-06602-x

Du, G.-X., Xue, Q., Ding, H., and Li, Z. (2015). Mechanochemical Effects of ZnO Powder in a Wet Super-fine Grinding System as Indicated by Instrumental Characterization. *Int. J. Mineral Process.* 141, 15–19. doi:10.1016/j.minpro.2015.06.008

Jaramillo-Páez, C., Navío, J. A., Hidalgo, M. C., and Macías, M. (2016). High UV-Photocatalytic Activity of ZnO and Ag/ZnO Synthesized by a Facile Method. *Catal. Today*, 284. doi:10.1016/j.cattod.2016.11.021

Jose, J., and Athikalam Paulose, S. (2020). Studies on Natural Rubber Nanocomposites by Incorporating Zinc Oxide Modified Graphene Oxide. *J. Rubber Res.* 23 (4), 311–321. doi:10.1007/s42464-020-00059-3

Kayış, A., Kavgacı, M., Yaykaşlı, H., Kerli, S., and Eskalen, H. (2021). Investigation of Structural, Morphological, Mechanical, Thermal and Optical Properties of PVA-ZnO Nanocomposites[J]. *Glass Phys. Chem.* 47 (5), 451–461. doi:10.1134/S1087659621050084

Kunio, E., and Meguro, K. (1975). The Effect of Grinding on the Surface Properties of Magnesia and Zinc Oxide[J]. *J. Jpn. Soc. Colour Mater.* 48 (9), 539–543.

Lehn, J. M., Wipff, G., and Demuynck, J. (1980). An Ab Initio Study of Stereoelectronic Effects in Zn(OH)42− and Zn(OH)2 Model Complexes. *Chem. Phys. Lett.* 76 (2), 344–346. doi:10.1016/0009-2614(80)87038-2

Lu, Jinfeng., Zhang, Qiwu., Wang, Jun., Saito, Fumio., and Uchida, Masashi. (2005). Synthesis of N-Doped ZnO by Grinding and Subsequent Heating ZnO-Urea Mixture[J]. *Powder Technology* 162 (1), 33–37. doi:10.1016/j.powtec.2005.12.007

Moballegh, A., Shahverdi, H. R., Aghababazadeh, R., and Mirhabibi, A. (2006). ZnO Nanoparticles Obtained by Mechanochemical Technique and the Optical Properties[J]. *Surf. Sci.* 601 (13), 2850–2854. doi:10.1016/j.susc.2006.12.012

Pronin, I. A., Yakushova, N. D., Sychev, M. M., Komolov, A. S., Myakin, S. V., Karmanov, A. A., et al. (2018). Evolution of Acid-Base Properties of the Surface of Zinc Oxide Powders Obtained by the Method of Grinding in an Attritor. *Glass Phys. Chem.* 44 (5), 464–473. doi:10.1134/s1087659618050140

Rui, Xiong., Shuanfa, Chen., Bowen, Guan., Yanping, Sheng., and Lu, Wang. (2014). Laboratory Investigation of Brucite Fiber in Stabilizing and Reinforcing Asphalt Binder[J]. *Int. J. Pavement Res. Technology* 7 (4), 256–262. doi:10.6135/ijprt.org.tw/2014.7(4).256

Scepanovic, M., Sreckovic, T., Vojisavljevic, K., and Ristic, M. M. (2006). Modification of the Structural and Optical Properties of Commercial ZnO Powder by Mechanical Activation. *Sci. Sinter* 38 (2), 169–175. doi:10.2298/sos0602169s

Sreethu, T. K., and Kinsuk, N. (2021). Zinc Oxide with Various Surface Characteristics and its Role on Mechanical Properties, Cure-Characteristics, and Morphological Analysis of Natural Rubber/carbon Black Composites[J]. *J. Polym. Res.* 28 (5), 1–14. doi:10.1007/s10965-021-02536-8

Sugavaneshwar, R. P., and Nanda, K. K. (2013). Ultralong ZnO Nanowires: Problems and Prospects. *Mat Express* 3 (3), 185–200. doi:10.1166/mex.2013.1125

Suthar, M., Panchal, M., and Patel, D. (2020). SYNTHESIS OF ZnO NANOPARTICLES AND ITS APPLICATIONS[J]. *Int. J. Adv. Res. (Ijar)* 8 (3). doi:10.21474/ijar01/10666

Tuan, A. N., Thi, Y. M., Truong, X. M. N., Ky, P. H. H., Minh, V. L., and Nguyen, T. A. N. (2020). Mechanochemical Synthesis of Zinc Oxide Nanoparticles and Their Antibacterial Activity against Escherichia Coli[J]. *Mater. Sci. Forum* 6044, 59–64. doi:10.4028/www.scientific.net/MSF.1007.59

Uekawa, N., Yamashita, R., Jun Wu, Y., and Kakegawa, K. (2004). Effect of Alkali Metal Hydroxide on Formation Processes of Zinc Oxide Crystallites from Aqueous Solutions Containing $Zn(OH)_4^2?$ Ions. *Phys. Chem. Chem. Phys.* 6 (2), 442–446. doi:10.1039/b310306d

Wang, D., Wang, H., and Di, S. (2019). Mechanical Properties and Microstructure of Magnesia-Fly Ash Pastes. *Road Mater. Pavement Des.* 20 (5), 1243–1254. doi:10.1080/14680629.2018.1439400

Wang, W., Xu, L., Xian, F., Yu, Z., Qian, H., Zhang, R., et al. (2020). Optical Properties of CuO/ZnO Composites Prepared by Mechanical Grinding. *Optik* 224, 165759. doi:10.1016/j.ijleo.2020.165759

Xu, M., and Wei, M. (2018). Layered Double Hydroxide-Based Catalysts: Recent Advances in Preparation, Structure, and Applications[J]. *Adv. Funct. Mater.* 28 (47), 1616–301X. doi:10.1002/adfm.201802943